Modulation of the Zinc(II) Center in Protein Farnesyltransferase by Mutagenesis of the Zinc(II) Ligands†

Christopher M. Harris, Aaron M. Derdowski, and C. Dale Poulter*

Department of Chemistry, University of Utah, Salt Lake City, Utah 84112

Received May 10, 2002

ABSTRACT: Protein farnesyltransferase (PFTase) is a zinc-containing metalloenzyme that catalyzes the alkylation of cysteine (C) in protein substrates containing a C-terminal "CaaX" motif by farnesyl diphosphate (FPP). In yeast PFTase Zn(II) is coordinated to D307, C309, and H363 in the β-subunit. The inner coordination sphere of the metal also contains a water molecule to give a net charge of 0 for the tetracoordinate Zn(II) center. When the protein substrate binds, the water molecule is replaced by the thiol of the cysteine residue, and the thiol is deprotonated to generate a Zn(II)-stabilized thiolate in the PFTase·FPP·protein ternary complex for the ensuing prenyl transfer reaction. An expression system was constructed for yeast PFTase containing a His_6 tag at the C-terminus of the β-subunit to facilitate purification of the wild-type enzyme and site-directed mutants. The amino acids that coordinate Zn(II) were substituted to give a series of mutant PFTases with net charges of +1, 0, −1, and −2 at the Zn(II) center of the ternary enzyme·substrate complexes. Wild-type PFTase and the site-directed mutants were purified as α,β-heterodimers, and each was found to contain an equivalent of Zn(II). All of the mutants were less reactive than wt PFTase (net charge of −1), with the greatest losses of activity seen for the mutants with net charges of 0 and +1. Equilibrium binding experiments with dGCVIA peptide and an unreactive analogue of FPP, (*E*,*E*)-2-[2-oxo-2-[[(3,7,11-trimethyl-2,6,10-dodecatrienyl)oxy]amino]ethyl]phosphonate (FNP), established that all of the mutants bound an equivalent of the peptide substrate. Like wt PFTase, the pH dependence of K_D for the mutants did not change significantly between pH 5 and pH 9, indicating that pK_As for the thiol moiety in the (mutant PFTase)·FNP·peptide complexes were <5. dGSVIA and dG-(β-NH_2-Ala)VIA, where the sulfhydryl moiety was replaced by hydroxyl and amino groups, respectively, were not substrates. These experiments suggest a direct relationship between the net charge of the Zn(II) center in PFTase and the reactivity of the peptide thiolate that is alkylated by FPP.

Protein farnesyltransferase (PFTase)[1] catalyzes alkylation of cysteine in CaaX sequences at the C-terminus of proteins and peptides by farnesyl diphosphate (FPP), where "C" is cysteine, "a" is a small hydrophobic amino acid, and "X" is A, S, M, or N, as illustrated in Scheme 1 (*1*). A closely related protein geranylgeranyltransferase type I (PGGTase I) adds a geranylgeranyl moiety from geranylgeranyl diphosphate when "X" is L or F (*2*, *3*). A third protein prenyltransferase, PGGTase II, catalyzes geranylgeranylation of two cysteines found within the four amino acids at the C-terminus of Rab proteins (*4*). These posttranslational modifications are necessary for the proteins to localize to the appropriate membrane surfaces in eukaryotic cells. Protein substrates for PFTase include Ras, nuclear lamins, yeast a-mating factor, Rho proteins, phosphorylase kinases, rhodopsin kinases, and many others (*5*). Farnesylation of oncogenic Ras is necessary for the protein to localize to the inner surface of the outer cellular membrane, where it exerts its transforming activity (*6*−*9*). Inhibitors of PFTase have completed phase 1 clinical trials as antitumor agents (*10*−*12*), and several phase 2 trials are underway.

Scheme 1: Reaction Catalyzed by Protein Farnesyltransferase

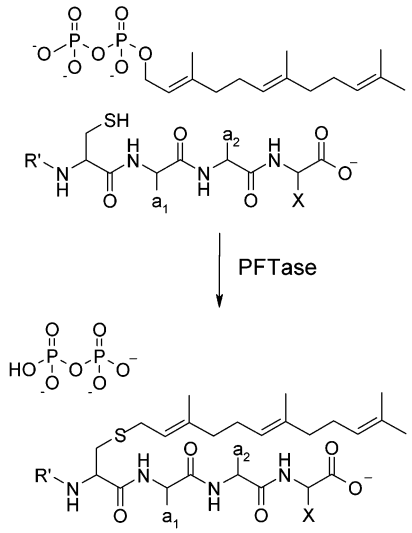

† This work was supported by National Institutes of Health Merit Award GM 21328 to C.D.P. C.M.H. is an NIH Postdoctoral Fellow (Grant GM20341). A.M.D. is a University of Utah Summer Undergraduate Fellow.

* To whom correspondence should be addressed.

[1] Abbreviations: dGCVIA, dansyl-Gly-Cys-Val-Ile-Ala; FPP, farnesyl diphosphate; FSPP, farnesyl thiolodiphosphate; orf, open reading frame; PFTase, protein farnesyltransferase; FNP, (*E*,*E*)-2-[2-oxo-2-[[(3,7,11-trimethyl-2,6,10-dodecatrienyl)oxy]amino]ethyl]phosphonic acid sodium salt; PGGTase I, protein geranylgeranyltransferase type I; wt, wild type.

10.1021/bi020349u CCC: $22.00
Published on Web 07/27/2002

PFTase is an α,β-heterodimer, and the β-subunit of the enzyme contains an essential tightly bound Zn(II) (*13*, *14*). In the resting state of PFTase, the Zn(II) is coordinated by aspartate, cysteine, and histidine residues, corresponding to D307, C309, and H363 in the *Saccharomyces cerevisiae* enzyme, and a fourth coordination site is occupied by a molecule of water (*15*, *16*). On the basis of X-ray structures of mammalian PFTases, the carboxylate in the aspartate side chain is ligated to Zn(II) in a bidentate fashion, and the resulting coordination geometry is distorted pentacoordinate. When the protein substrate binds, the zinc-bound water is replaced by the cysteine thiol in the C-terminal CaaX motif (*17*, *18*). The sulfhydryl proton is then removed to form the enzyme-bound Zn(II) thiolate (*19*, *20*).

Coordination of water or thiols to Zn(II) increases the acidity of the attached protons. The magnitude of the change depends on the other ligands attached to the metal. Ab initio calculations of Zn(II)$-OH_2$ and Zn(II)$-$OH complexes suggest that the pK_A of the bound ligand decreases approximately 3 units each time the net charge of the complexes changes by $+1$ (*21*). In carbonic anhydrase where an active site zinc is coordinated to three histidines, the water in the active site $[Zn(his)_3H_2O]^{2+}$ complex has a pK_A of $\sim$7 **(***22***)**. The dramatic decrease in the pK_A of the bound water molecule facilitates formation of the zinc$-$hydroxide complex needed for the hydration of CO_2, and the Zn(II) complex with a net charge of $+2$ appears to be optimal for catalysis. When the active site histidines are replaced by amino acids with negatively charged side chains, the activity of the enzyme decreases substantially (*23*).

PFTase binds its substrates in an ordered sequence with FPP preceding the protein substrates. Like carbonic anhydrase, PFTase uses Zn(II) to lower the pK_A of the nucleophilic partner in the reaction. Upon binding to the enzyme, the pK_A of the CaaX cysteine residue in the protein substrate is lowered from $\sim$9 to $\leq$5. The cysteine thiol is rapidly deprotonated to give a zinc-bound thiolate in a Zn(II) complex with a net charge of -1 (*17*, *19*, *20*). We have altered the net charge of the Zn(II) cluster by site-directed mutagenesis of the amino acids in the inner coordination sphere of the zinc atom and find that a cluster with a net charge of -1 in the ternary enzyme·substrate complex appears to be an optimal combination for deprotonating the thiol while maintaining the nucleophilicity of the thiolate in the prenyl transfer reaction.

MATERIALS AND METHODS

Materials. FPP was synthesized by the method of Davisson (*24*). Dansyl peptides and DNA primers were synthesized by Dr. Robert Schackmann at the University of Utah Core Facility. Sodium (*E*,*E*)-2-[2-oxo-2-[[(3,7,11-trimethyl-2,6,-10-dodecatrienyl)oxy]amino]ethyl]phosphonate (FNP) was purchased from Calbiochem. All other materials were purchased from Sigma, except where stated otherwise.

Mutagenesis. Site-directed mutagenesis of *S. cerevisiae* PFTase was performed using the Promega GeneEditor system. Plasmid pGP14 (*25*) was purified from DH5α *Escherichia coli* cells by Qiagen Midi Prep. This plasmid contains two copies of RAM2 (encoding the α-subunit) with a copy of RAM1 (β-subunit) in between. All mutations introduced in this study were in the β-subunit. Mutagenesis primers are listed in Table 1. In addition to the mutations of interest, primers introduced silent mutations to add an *Alu*I site, for mutations at D307 or C309, or a *Mae*I site, for mutations at H363. Mutations were screened by restriction analysis with *Alu*I or *Mae*I and by dideoxy nucleotide sequencing at the University of Utah Core Facility. The entire RAM1 gene and both copies of RAM2 were sequenced to confirm the absence of spurious mutations.

Protein Expression and Purification from pGP14. Plasmids encoding the appropriate PFTases were transformed into chemically competent JM101 *E. coli* cells and were grown on LB/ampicillin plates. Individual colonies were used to inoculate six 3 mL cultures of LB with 100 μg/mL ampicillin. The slowest growing cultures were used to inoculate large cultures. At least two different starter cultures were used to inoculate six 2 L flasks, each containing 500 mL of SB media and 100 μg/mL ampicillin. Cultures were grown at 37 °C for 15 h with shaking at 250 rpm. Cells were harvested by centrifugation and stored at -80 °C for up to 4 weeks. Typically, 22$-$25 g of wet cell paste was collected from 3 L of culture. Protein purification was performed as described previously (*15*, *25*). Approximately 0.5$-$1 mg of >90% pure enzyme was obtained per liter of culture.

Construction of pET24-RAM2/RAM1. The open reading frames (orf's) for wt RAM2 and RAM1 proteins were subcloned into a pET expression vector in order to append a His_6 sequence to the C-terminus of the RAM1 protein and facilitate PFTase purification. A 2284 bp fragment from pGP14 containing RAM1 and the 5′ copy of RAM2 was amplified by PCR. The forward primer contained 47 bases, 34 of which were complementary to the vector sequence upstream of the 5′ copy of RAM2 and 13 of which were complementary to the 5′ end of RAM2: 5′-AACATAT-TGTTAACTTTACATGACAGGAGTACATATGGAGGAG-TACG-3′. The RAM2 start codon is indicated in bold, and an *Nde*I site is underlined. The reverse primer contained 31 bases, 22 of which were complementary to the 3′ end of

Table 1: Primers Used for Site-Directed Mutagenesis[a]

mutant	mutagenic primer
D307H	AGCAACAAACTTGTT*CAC*GG**A**TG**T**TATAGCTTTTGGGTTGGAGG
D307C	AGCAACAAACTTGTT*TGC*GG**A**TG**T**TATAGCTTTTGGGTTGGAGG
C309H	AAACTTGTTGACGGT*CAC*TATAGCTTTTGGGTTGGAGG
3His (D307H, C309H)	AGCAACAAACTTGTT*CAC*GGT*CAC*TATAGCTTTTGGGTTGGAGG
H363E	CACTCAGACTTTTAC*GAA*ACAAATTATTGCCTACTAGGACTGGCTGTTGCG
H363C	CACTCAGACTTTTAC*TGT*ACAAATTATTGCCTACTAGGACTGGCTGTTGCG
3Cys (D307C, H363C)	AGCAACAAACTTGTT*TGC*GG**A**TG**T**TATAGCTTTTGGGTTGGAGG and CACTCAGACTTTTAC*GAA*ACAAATTATTGCCTACTAGGACTGGCTGTTGCG

[a] The new codon is indicated in italics. Mutants contain the primer sequence on the sense strand. Silent mutations were introduced to reduce primer secondary structure (bold) and to introduce an *Alu*I or a *Mae*I site (underlined). All mutations are in the β-subunit.

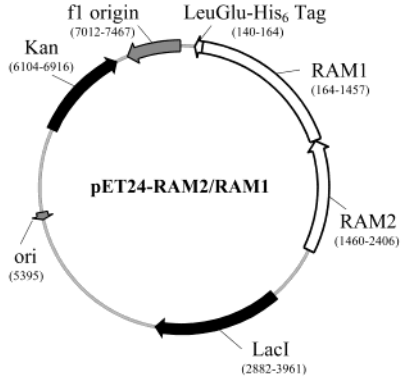

FIGURE 1: Expression plasmid pET24-RAM2/RAM1.

RAM1: 5′-**CCG**CTCGAGCTGTGGAGAAGATAAATTG-GAT-3′. The reverse primer removed the C-terminal EEF anti-α-tubulin epitope previously used for immunoaffinity chromatography (*25*). In its place, a *Xho*I site was introduced (underlined), encoding LE, plus 3 bases, CGG (bold), to facilitate subsequent *Xho*I digestion. The PCR product was purified on a 1% agarose gel and extracted from the gel using the Qiagen QIAEX II system. The purified DNA was ligated into pGEM T-easy (Promega), and the resulting circular pGEM-RAM2/RAM1 construct was transformed into chemically competent XL1-Blue cells. Transformants were selected by growth on ampicillin. pGEM-RAM2/RAM1 was purified from XL1-Blue cells by the Promega Wizard protocol. Sequence analysis of pGEM-RAM2/RAM1 indicated that the RAM2/RAM1 module was free of mutations and was inserted in the opposite orientation as the plasmid's T7 promoter. Plasmids pGEM-RAM2/RAM1 and pET24a(+) (Novagen) were separately digested with *Nde*I and *Xho*I and gel purified to obtain the 2249 bp RAM2/RAM1 fragment and the 5234 bp linear pET24a(+) vector, respectively. The two fragments were ligated and transformed into XL1-Blue cells. Cells were selected for growth on kanamycin. Restriction analysis and sequencing confirmed the desired construct. Ligation of the RAM2/RAM1 module into pET24a(+) yielded pET24-RAM2/RAM1 (Figure 1) with the RAM2 and RAM1 orf's under control of the T7 promoter and a His_6 tag appended to the C-terminus of the RAM1 protein. Both genes utilize the same T7 promoter, upstream of RAM2. Due to problems expressing the C309H mutant from pGP14, the genes encoding this enzyme were also subcloned into pET24a(+) by the same procedure as for wild type.

Expression and Purification from pET24-RAM2/RAM1. Vector pET24-RAM2/RAM1 was transformed into chemically competent Epicurian coli BL21(DE3) Codon Plus RIL cells (Stratagene). Starter cultures (3 mL of LB, 30 μg/mL kanamycin, 34 μg/mL chloramphenicol) were grown overnight at 37 °C, with shaking. Two cultures, each containing 500 mL of LB, 30 μg/mL kanamycin, 34 μg/mL chloramphenicol, and 100 μM $ZnSO_4$, were inoculated with 1 mL of the overnight culture and were grown at 37 °C, with shaking at 240 rpm, until $OD_{600} = 0.8$. IPTG was added to 1 mM (final concentration), incubation was continued for 3 h, and cells were harvested by centrifugation and stored at −80 °C.

Cell paste (4.5 g) was resuspended in 18 mL of 50 mM sodium phosphate, pH = 8.0, 300 mM NaCl, 20 mM imidazole, 1 mM β-mercaptoethanol, and 1 mM phenylmethanesulfonyl fluoride (PMSF). Cells were lysed by sonication, three periods of 30 s each. The sample was centrifuged for 30 min at 18000 rpm in a Beckman J20 rotor. The supernatant was loaded onto 1.8 mL Ni-NTA agarose resin (Qiagen) in a 0.5 × 14 cm Pharmacia column that had been preequilibrated in sonication buffer without PMSF, at a flow rate of 0.5 mL/min. The column was washed with sonication buffer (minus PMSF) at 1 mL/min until the absorbance at 280 nm reached a minimum, about 50−60 mL. PFTase was eluted with a linear gradient from 20 to 500 mM imidazole, at a flow rate of 1 mL/min. Column fractions were screened for activity and by SDS−PAGE. Pooled fractions were dialyzed four times against 50 mM Tris, pH = 7.0, and 10 mM β-mercaptoethanol. Significant activity was lost when PFTase was left overnight in the elution buffer. This was circumvented by initiating dialysis soon after elution. Dialyzed enzyme was concentrated in a Centriprep-10 unit (Amicon), centrifuged 30 min at 18000 rpm to remove particulate matter, made 30% with respect to glycerol, partitioned into small tubes, and flash frozen in liquid nitrogen. Samples were stored at −80 °C. One liter of cell culture resulted in up to 4.5 g of wet cell paste and up to 14 mg of PFTase that was at least 95% pure by SDS−PAGE (Figure 2). Enzyme had a specific activity of 0.045 μmol s^{-1} mg^{-1} in the fluorescence assay (see below). Similar results were obtained by using Ni-NTA silica resin (Qiagen).

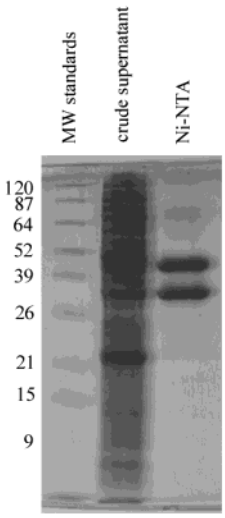

FIGURE 2: Purification of wild-type His_6 PFTase by 12% SDS−PAGE.

Protein Concentration. Approximately 0.8 mg of wild-type PFTase was dialyzed three times against 300 mL 10 mM sodium phosphate, pH 7.5. Protein concentration was determined by Bradford analysis, by amino acid analysis (performed by Dr. Dennis Winge, University of Utah), and by extinction at 280 nm.

Zn(II) Analysis. Enzymes were analyzed for Zn(II) content by a modification of an earlier procedure (*15*). Metal-free buffer solutions were prepared by stirring for 5 h with 50 g of Chelex-100 resin (Bio-Rad) per liter of buffer. The resin was removed by filtration. Approximately 15 nmol of enzyme (0.5−2.5 mL total) was dialyzed three times against 1 L of metal-free 50 mM Tris-HCl, pH 7.0, containing 50 g of Chelex-100. After dialysis, the samples were concentrated to ∼1 mL in Centricon-10 units (Amicon) to a final concentration of ∼15 μM. Samples were centrifuged at

14000 rpm for 20 min to remove any precipitate, and protein concentrations were determined by Bradford analysis. Samples were flash-frozen in liquid nitrogen. Zn(II) analysis was performed by ICP atomic absorption spectroscopy at The Chemical Analysis Laboratory, University of Georgia.

Steady-State Kinetic Measurements. Activity was measured by the increase in fluorescence intensity upon farnesylation of dansyl-Gly-Cys-Val-Ile-Ala (dGCVIA) (*26*, *27*). Assays were performed at 30 °C in a buffer consisting of 50 mM Tris-HCl, pH 7.0, 0.04% *n*-dodecyl β-D-maltoside, 10 mM $MgCl_2$, 5 mM DTT, and 10 μM $ZnCl_2$. For standard assays, the buffer contained 20 μM FPP, 2.4 μM dGCVIA, and 5−100 nM enzyme. Steady-state kinetic analyses were performed on the purified mutants by varying the concentration of one substrate at a saturating concentration of the second. In cases where substrate inhibition by the peptide was seen (*28*), the FPP concentration was varied at a fixed peptide concentration that resulted in maximal activity. Steady-state data were fit by nonlinear least-mean-squares procedures with the Kaleidagraph program (Spectrum Software Associates) according to eq 1 for normal Michaelis−Menten behavior or to eq 2 for substrate inhibition:

$$\frac{v}{[E_{tot}]} = \frac{k_{cat}[S]}{K_m + [S]} \quad (1)$$

$$\frac{v}{[E_{tot}]} = \frac{k_{cat}[S]}{K_m + [S](1 + [S]/K_i)} \quad (2)$$

Peptide Binding Assay. Equilibrium dissociation constants, K_D, for dGCVIA were measured by fluorescence energy transfer, exciting enzyme tryptophan at 280 nm and measuring emission from bound dGCVIA at 496 nm (*19*). Samples contained 0.5 μM enzyme, 5 μM sodium (*E*,*E*)-2-[2-oxo-2-[[(3,7,11-trimethyl-2,6,10-dodecatrienyl)oxy]amino]ethyl]-phosphonate (FNP), 5 mM DTT, 5 mM $MgCl_2$, 0.04% *n*-dodecyl β-D-maltoside, 26 mM MES, 26 mM TAPSO, and 50 mM diethanolamine, in an initial volume of 200 μL. Small volumes of dGCVIA solutions were added serially. Experiments were performed at 30 °C. Fluorescence emission at 496 nm was corrected for dilution and for background emission of unbound dGCVIA and normalized to zero with respect to the initial emission. K_D values were close in magnitude to [E]. Since $[dGCVIA_{free}]$ cannot be assumed to equal $[dGCVIA_{tot}]$, data were fit to the equation:

$$\Delta Em_n^{496} = \frac{\Delta Em_{tot}^{496}}{2[E]}[([E] + [dGCVIA] + K_D) - \sqrt{([E] + [dGCVIA] + K_D)^2 - 4[E][dGCVIA]}] \quad (3)$$

Analysis was performed using nonlinear least-mean-squares curve fitting with the Kaleidagraph program (Spectrum Software Associates).

RESULTS

Mutations in PFTase That Alter the Ligands Bound to Zn(II). PFTase mutants were designed to vary the net charge of the Zn(II) center while still utilizing ligands likely to bind Zn(II) with high affinity. Wherever possible, combinations of ligands were chosen to correspond to those used in other Zn(II)-containing enzymes. Net charges for the Zn(II) center are given as the charge in the presence of ionized peptide substrate. All residues mutated were on the β-subunit. The D307H/C309H (3His) double mutant has three histidines for binding Zn(II), a motif found in carbonic anhydrase (*29*), and a metal center with a +1 charge. D307H and C309H mutants should have a neutral Zn(II) center. In the case of D307H, the resulting Cys, His, His combination is similar to the Zn(II) binding motif in carboxypeptidase A (*30*). For C309H, the Asp, His, and His environment for Zn(II) is similar to the metal binding sites in alcohol dehydrogenase and cytidine deaminase (*31*, *32*). D307C was chosen as a positive control that has the same net charge at the Zn(II) center as wt PFTase. The H363E, H363C, and D307C/H363C (3Cys) mutants each have a −2 charge at zinc in the enzyme·substrate complex. The Zn(II) site in the 3Cys double mutant resembles the Ada protein (*33*).

The mutations were selected after molecular modeling based upon the crystal structure of rat PFTase (*16*). With two exceptions, modeling indicated appropriate Zn(II)−ligand bond distances. For C309H, the histidine can only be accommodated with Zn(II) parallel, not orthogonal, to the imidazole ring, and some reorganization within the protein would be necessary for this side chain to ligate Zn(II). In the case of H363C, modeling indicates the Zn(II)−sulfur bond distance would be 4.2 Å, and adjustments in the protein scaffold would be necessary to move the sulfur to the 2.2 Å distance seen in rat PFTase (*16*).

Construction of pET24-RAM2/RAM1. Most of the mutagenesis experiments were conducted with pGP14, an expression plasmid that contained two copies of RAM2 and a copy of RAM1 with codons for a Glu-Glu-Phe α-tubulin epitope appended to the 3′-end of the orf to facilitate purification by immunoaffinity chromatography (*25*). When we experienced problems with expression of the protein for the C309H mutant, a new expression system was developed for wt and C309H PFTase (Figure 1). PCR was used to obtain a fragment from pGP14. The upstream primer mostly complemented the upstream vector region to avoid annealing to the second copy of RAM2. The downstream primer was complementary to the 3′-end of RAM1 and introduced a *Xho*I site. The junction of RAM2 and RAM1 is unchanged from pGP14, where the stop codon for RAM2 overlaps with the start codon for RAM1 (TGATG). A His_6 tag was also appended to the ram1 protein to give a C-terminal LSSPQLE-HHHHHH sequence. Wt ram1 protein ends with LSSPS.

Expression and Purification. PFTase mutants were originally constructed in pGP14 (*25*). Production of mutants from the pGP14 system was sufficient to recover 1−3 mg of enzyme at ≥90% purity, although the lower levels of production of the mutants relative to wt enzyme required two ion-exchange columns (*15*, *25*) before the immunoaffinity chromatographic step in order to obtain pure enzyme. However, the characteristic bands for the α- and β-subunits were not seen on an SDS gel of the mutant C309H nor was the protein detected by Western blots (data not shown) using anti-EEF rat IgG (*25*).

A new expression plasmid was constructed that contained single copies of RAM1 and RAM2 to facilitate possible mutagenesis of the α-subunit and that appended a His_6 tag to the ram1 protein for purification by chromatography on a Ni(II) column. The ram2/ram1 module was expressed in

Table 2: Purification of PFTase-His_6 from pET24-RAM2/RAM1

sample	volume (mL)	[protein] (mg/mL)	total protein (mg)	activity (μmol s^{-1} mL^{-1})	total act. (μmol s^{-1})	act. yield (%)	sp act. (μmol s^{-1} mg^{-1})
crude extract	20	13	250	0.063	1.2	100	4.9×10^{-3}
Ni-NTA	1.1	13	14	0.58	0.63	52	0.045

Table 3: Stoichiometry of Zn(II) Binding[a]

enzyme	equiv of Zn(II)	enzyme	equiv of Zn(II)
wild-type His_6	0.9[b]	D307C	0.9[c]
	0.4[c]	H363C	0.7[c]
3His	0.8[c]	H363E	0.1[c]
C309H	0.4[c]	3Cys	0.8[c]
D307H	0.2[c]		

[a] Enzyme concentration was determined by Bradford analysis. Zn(II) concentration was determined by ICP atomic absorption spectroscopy. All mutated residues are on the β-subunit. These values reflect a time-dependent loss of Zn^{2+} during dialysis (see Results). [b] 2 h dialysis.[c] 24 h dialysis.

Epicurian coli BL21 Codon Plus RIL cells, a strain that contains tRNA genes for codons not normally used in *E. coli*. Together, RAM1 and RAM2 contain 59 such codons. SDS−PAGE gels of crude extracts showed that induction with IPTG resulted in a large increase in expression of the α- and β-subunits, which reached a plateau from 3 to 6 h after induction (not shown). Purification of supernatant from a crude homogenate was completed in a single chromatographic step on Ni-NTA. SDS−PAGE indicated the material was >95% pure (Figure 2.). Fractions from the Ni-NTA column lost most of their activity when left in elution buffer overnight at 0 °C. However, activity was retained when the samples were dialyzed against 50 mM Tris, pH = 7.0, and 10 mM β-mercaptoethanol. These samples could be stored at −80 °C for up to 9 months with no detectable loss in activity. The specific activity of 0.045 μmol s^{-1} mg^{-1}, measured at standard assay conditions of 20 μM FPP and 2.4 μM dGCVIA, is similar to the published value of 0.057 μmol s^{-1} mg^{-1} (*28*).

The new purification only requires one step, provided approximately 14 mg of enzyme in 52% yield from a 1 L culture (see Table 2), and replaces the immunoaffinity step with a Ni(II) column. Other efficient expression systems were recently reported for rat PFTase (*34*, *35*). The C309H mutant was also expressed in good yield from a pET24a construct and purified as described for the wt enzyme.

Zn(II) Content. Purified mutants were analyzed for their Zn(II) content by ICP atomic absorption spectroscopy, and the results are listed in Table 3. Several methods for measuring the protein concentrations of our samples were compared using wt PFTase. The concentrations measured by the Bradford procedure and by amino acid analysis agreed within the experimental error, suggesting that no correction was required for the Bradford determination. The extinction coefficient of PFTase at 280 nm based on concentrations from by Bradford determinations ($\epsilon = 1.32 \times 10^5$ M^{-1} cm^{-1}) was only slightly below the calculated value ($\epsilon = 1.53 \times 10^5$ M^{-1} cm^{-1}) based on the aromatic amino acids in yeast PFTase (*36*).

The values in Table 3 are lower than anticipated. We found the specific activity of the wt His_6 enzyme decreased during dialysis against Chelex resin in a first-order fashion with a $t_{1/2} = 20$ h (data not shown). We attribute the loss of activity to loss of Zn(II). When dialyzed against metal-free buffer lacking Chelex, the first-order loss of enzyme activity slowed with a $t_{1/2} = 43$ h, and when dialyzed against buffer containing 100 μM $ZnCl_2$, no measurable loss of activity was observed. The specific activity of the dialyzed samples did not change when they were incubated with buffer containing 100 μM $ZnCl_2$ for up to 24 h at 0 °C. The loss of catalytic activity was accompanied by loss of Zn(II). Samples of wt His_6 PFTase were dialyzed for 2 and 24 h against metal-free buffer and Chelex and subjected to metal analysis. After dialysis for 2 h, the enzyme contained 0.9 equiv of Zn(II), whereas the Zn(II) content was reduced to 0.4 equiv at 24 h. The loss of Zn(II) closely paralleled the loss of specific activity. The specific activity of the H363E mutant was also monitored as a function of dialysis time. This enzyme lost activity significantly faster than the wt-His_6 enzyme ($t_{1/2} = 2.5$ h). After dialysis for 24 h, the H363E mutant only contained slightly less than 0.1 equiv of Zn(II). Our data suggest that the substiochiometric concentrations of Zn(II) seen in Table 3 result from loss of the metal during dialysis and that loss of Zn(II) results in a corresponding reduction in the specific activities of the enzymes. Thus, the Zn(II) stoichiometries in Table 3 should be regarded as minimal values. The wt and mutant PFTases retained activity for extended periods of time when stored in buffers containing Zn(II). Since $ZnCl_2$ was included in the buffers used for purification of the proteins and the subsequent assays, it is reasonable to assume that the differences in kinetic behavior seen for the wt and mutant proteins are not due to differences in Zn(II) content.

Steady-State Kinetics. Steady-state kinetic parameters for wt PFTase and the mutants are reported in Table 4. Wt PFTase shows substrate inhibition when [FPP] is held constant and [peptide] is varied, as illustrated in Figure 3 for the His_6 version of the protein. All of the mutants also showed substrate inhibition except for D307H and 3Cys, which gave normal Michaelis−Menten behavior. There were no significant changes in k_{cat} for wt PFTase when the C-terminal EEF motif in the β-subunit was replaced with a His_6 tag, although K_M and K_I were slightly elevated in wt His_6. Two of the PFTase mutants, H363C and 3His, had no measurable activity, although as seen in Tables 2 and 4, both proteins were able to bind Zn(II) and dGCVIA. H363C is one of three mutants with a charge of −2 at the Zn(II) center when peptide is bound in the thiolate form. Since the two other mutants, H363E and 3Cys, are active, factors other than net charge of the center must be responsible for the lack of activity for the H363C protein. As mentioned earlier, the predicted distance between the sulfur in Cys363 and the zinc is approximately 2 Å longer than the H363(nitrogen)−Zn(II) distance in wt PFTase (*16*), and a substantial movement of residues in the protein is necessary to bring the

Table 4: Steady-State Kinetic Parameters for Mutant PFTases[a]

enzyme	net charge Zn(II) center	k_{cat} (s^{-1})	K_M, FPP (μM)	K_M, peptide (μM)	K_I, peptide (μM)
3His	1+	not detected			
C309H	0	1.2×10^{-3}	nd[c]	nd[c]	nd[c]
D307H	0	0.0032 ± 0.0008	0.21 ± 0.03	1.3 ± 0.4	na[c]
wild-type EEF[b]	1−	4.5 ± 1	1.7 ± 0.5	0.9	1.1
wild-type His_6	1−	3.8 ± 1.3	2.4 ± 0.6	3.7 ± 1.7	4.7 ± 2.3
D307C	1−	0.21 ± 0.03	1.9 ± 0.3	9.5 ± 2.8	85 ± 31
H363C	2−	not detected			
H363E	2−	0.40 ± 0.02	5.0 ± 1.1	34 ± 8	190 ± 50
3Cys	2−	0.021 ± 0.007	470 ± 210	33 ± 3	na[d]

[a] All mutated residues are on the β-subunit. Measurements were made using the fluorescence assay (*26*, *27*) at 30 °C. [b] Values taken from ref *28*. [c] Not determined. [d] Not applicable.

Table 5: Equilibrium Binding of dGCVIA Peptide to PFTases[a]

enzyme	net charge Zn(II) center	K_D (dGCVIA) (nM)
3His	1+	240 ± 90
C309H	0	130 ± 50
D307H	0	290 ± 140
wild-type His_6	1−	450 ± 30
D307C	1−	34 ± 18
H363C	2−	210 ± 60
H363E	2−	5−20
H363E-FNP	2−	350 ± 70
3Cys	2−	90 ± 50

[a] Values were measured as in Figure 4. Errors represent the standard deviation from multiple measurements. A range of values is given for H363E, and this represents plausible boundaries for K_D, based upon simulations to eq 3.

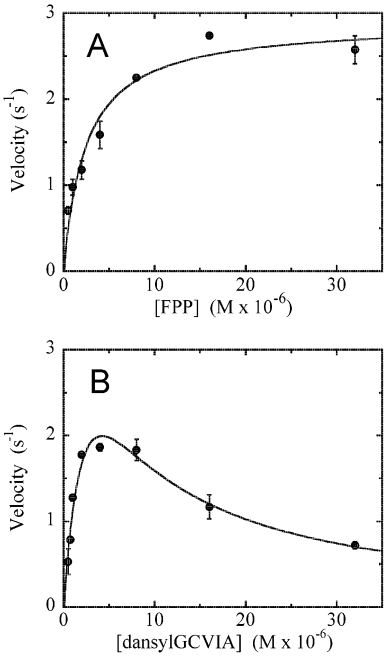

FIGURE 3: Steady-state kinetics of wild-type His_6 PFTase. Measurements were made by the method of initial rates using the fluorescence assay (see Materials and Methods) at 30 °C. Velocity is expressed as μM product s^{-1} μM enzyme^{-1}. Data in panel A were fit to eq 1; data in panel B were fit to eq 2. Fitted parameters are given in Table 4. Enzyme concentration is 3.4 nM.

thiolate and the zinc atom to within an optimal distance. It is possible that the catalytic site of the H363C mutant is too distorted for efficient catalysis. The other inactive mutant, 3His, has a +1 Zn(II) center when the thiolate form of the peptide is bound. Since this is the only +1 mutant studied, it is not possible to determine if its inactivity is due to reduced nucleophilicity of the protein thiolate or structural perturbations in the enzyme−substrate complex. We attribute the differences in k_{cat} reported in Table 4 to intrinsic properties of the Zn(II) metalloproteins rather than difference in their Zn(II) content. The difference in specific activities between wt PFTase and the least reactive mutant is greater than ~1000-fold. The range of specific activities is far greater than that for loss of Zn(II) we observed. Although product dissociation is the rate-limiting step for yeast PFTase, the chemical step is only ~3 times faster (36). It is unlikely that the large reductions in turnover observed in this study result from an even slower rate for product release. Thus, we assume that the k_{cat} values for the mutants listed in Table 4 represent the chemical step.

In general, the activity of the mutants increased as the Zn(II) center became more negative. The C309H and D307H enzymes, with a neutral Zn(II) center in the enzyme−substrate complex, are ≥300-fold less active than the wt enzyme. However, the low values of K_M for FPP and of K_M and K_I for the peptide substrates suggest that binding has not been substantially compromised. The D307C mutant·substrate complex has the same charge at the Zn(II) center as wt PFTase. In this case, replacement of the carboxylate moiety in aspartate by a cysteine thiolate only reduces k_{cat} by ~18-fold. The mutants, H363E and 3Cys, with −2 Zn(II) centers in their respective ternary enzyme·substrate complexes are active. Although the K_Ms for FPP and peptide are somewhat elevated for both mutants, k_{cat} for H363E is only 10-fold lower than wt and is *higher* than k_{cat} for the D307C enzyme, which has the same net charge at the Zn(II) center as wt PFTase.

Ionization of Bound Peptide. A series of equilibrium binding experiments were performed to determine the effect of net charge at the Zn(II) center on the pK_A of the bound peptide thiol. Binding of dGCVIA was measured by fluorescence energy transfer, with excitation of an enzyme tryptophan at 280 nm and measuring dansyl emission at 496 nm (*19*), in buffer containing $MgCl_2$ and an unreactive analogue of FPP, FNP. Two control experiments were conducted to establish the validity of the binding protocol. Changes in the enzyme concentration resulted in the same K_D with concomitant changes in the total emission at 496 nm, and nonfluorescent peptide RTRCVIA competed with dGCVIA to reduce the intensity of dansyl emission (not shown). In all of the experiments the enzyme concentration did not exceed twice K_D. Binding curves were fit according to eq 3, and a representative example is shown in Figure 4.

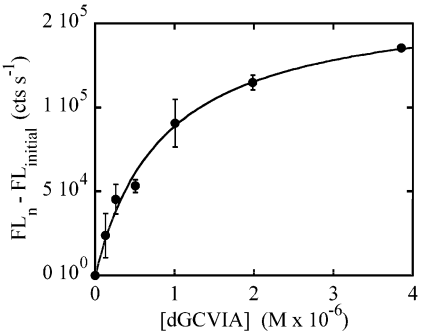

FIGURE 4: Binding of dGCVIA peptide to wild-type His_6 PFTase at pH 7.0. Serial additions of dGCVIA were made to a 200 μL solution of 0.5 μM PFTase. Emission intensity at 496 nm was measured, with excitation at 280 nm, corrected for unbound dGCVIA, and normalized to zero initial emission. Data were fit to eq 3 to give a $K_D = 450 \pm 30$ nM and a total emission increase of 150000 ± 300 counts s^{-1}.

The K_Ds measured for dGCVIA in this study were somewhat lower than those reported previously for other peptides using a fluorescence anisotropy assay (*20*). Tighter peptide binding may be due to the use of the tight-binding FPP analogue, FNP. A similar effect on GCVLS binding was observed for this analogue with rat PFTase (*37*). For wt PFTase and all of the mutants, K_D was independent of pH for $5 < pH < 9$ (data not shown). These results indicate that the peptide substrate was bound as a thiolate for all of the proteins, regardless of the net charge at the Zn(II) center, over the range of pHs.

Peptide binding experiments were repeated using a fluorescence polarization anisotropy assay developed by Rozema and Poulter (20). Farnesyl thiolodiphosphate (FSPP), an isoelectronic and essentially isosteric analogue of FPP, was used as a replacement for the normal substrate. FSPP binds tightly to wt PFTase with $K_D = 36$ nM and is essentially inert during the time required for the binding measurements. K_Ds were measured for difluorocarboxyfluorescein-RTRCVIA (flRTRCVIA) using fluorescence anisotropy. K_Ds for 3-mercaptopropanoyl-VIA (thiol $pK_a = 9.7$) were determined by competition with flRTRCVIA (*20*). Measurements were conducted with wt His_6 PFTase and the H363E mutant between pH 6 and pH 9. The results for both enzymes were similar to those reported above for dGCVIA binding.

In contrast to yeast PFTase, the pK_A of the bound water in carbonic anhydrase was highly dependent on the charge of the Zn(II) ligands (*23*). Thus, the Zn(II) in a cluster with one neutral and two negatively charged ligands in PFTase is a sufficiently strong Lewis acid to lower the pK_A of peptide thiol below 5, while the Zn(II) in carbonic anhydrase needed three neutral ligands to reduce the pK_A of the bound water to 7.

Activity with Peptides Containing Oxygen and Nitrogen Nucleophiles. The peptides dGSVIA and dG(L-β-NH_2-Ala)-VIA were tested as alternate substrates to see if nucleophiles other than sulfur were active in the prenyl transfer reaction for PFTase mutants with neutral or positively charged Zn(II) clusters. Neither wt PFTase nor any of the mutants catalyzed alkylation of the serine hydroxyl group in dGSVIA or the amino group in dG(L-β-NH_2-Ala)VIA. In addition, both compounds are very poor inhibitors, having IC_{50} values greater than 500 μM.

DISCUSSION

Several chemical properties of Zn(II) are important for its broad use as a cofactor in biocatalysis. Zn(II) is moderately polarizable and can adopt a variety of coordination geometries of similar energy. This allows the metal to coordinate with both hard and soft ligands in a protein scaffold and to bind in a variety of active site geometries (*38*). Zn(II) is a Lewis acid, undergoes ligand exchange rapidly, and is not redox active at physiological potentials (*38*). Enzymes exploit these characteristics to catalyze a variety of reactions. For example, alcohol dehydrogenase and L-fruculose-1-phosphate aldolase use Zn(II) as a Lewis acid to stabilize oxyanions during hydride transfer and aldol condensations (*31*, *39*). Carbonic anhydrase and adenosine deaminase lower the pK_A of a bound water molecule by coordination with Zn(II) to generate a nucleophilic hydroxide ion at physiological pH (*29*, *40*). Enzymes such as carboxypeptidase A and alkaline phosphatase appear to use a combination of these effects to enhance the electrophilicity of their substrates while assisting with formation of the nucleophile (*30*, *41*).

Many of the nucleophiles used in enzyme-catalyzed reactions are protonated at neutral pH and are much less reactive than the corresponding conjugate bases (*42*, *43*). Enzymes stabilize the more nucleophilic conjugate bases by a variety of means, including the polarity of the microenvironment, orientation, hydrogen bonding, and chelation to metals. However, the interactions that stabilize the conjugate bases can also reduce their nucleophilicity. An example of this phenomenon was recently encountered by Wilker and Lippard during a model study of Ada methyl phosphotriester repair center, a repair protein that transfers the methyl group from the phosphotriester to a cysteinyl thiolate in a $[Zn(cys)_4]^{2-}$ cluster of the protein (*44*, *45*). In the model studies benzenethiol was not sufficiently nucleophilic to demethylate trimethyl phosphate at a measurable rate, while under similar conditions the reaction proceeded rapidly with the corresponding tetraalkylammonium thiolate. However, when the thiolate was attached to Zn(II) in benzenethiolate or benzenethiolate/methylimidizole complexes, its nucleophilicity decreased dramatically. In fact, only the tetramethylammonium salts of $[Zn(II)(benzenethiolate)_4]^{2-}$ and $[Zn(II)(benzenethiolate)_3(methylimidazole)]^-$ gave measurable rates of demethylation. This study indicated that a dissociated thiolate was the active species in the displacement reactions and that the differences in reactivity reflected differences in the equilibrium concentration of free thiolate (see Scheme 2).

Scheme 2: Zn(II) Activation of Nucleophiles

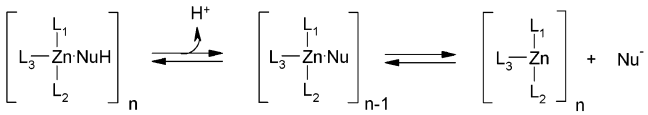

As the net charge increases from -1 to $+1$, the thiolate·imidazole complexes are less prone to dissociation and are less reactive. Thus, although coordination of a sulfhydryl group to zinc facilitates its deprotonation, the resulting zinc-bound thiolate is substantially less nucleophilic than its "free" counterpart.

The influence of zinc coordination on nucleophilic catalysis has been studied for carbonic anhydrase and Zn(II)

hydrolases (*29*, *30*, *40*). The Zn(II)−oxygen bond and, to a lesser extent, protein·ligand interactions provide approximately 9.5 kcal mol^{-1} of stabilization and lower the pK_A of water by ~7 pH units to physiological levels. Despite the strength of this interaction, dissociation of hydroxide from the coordination sphere of Zn(II) is sufficiently fast to support a diffusion-controlled k_{cat} for carbonic anhydrase (*29*). Zn(II) hydrolases and hydratases activate water for nucleophilic attack and have positively or neutrally charged Zn(II) centers. A recent review by Lipscomb and Strater (*46*) lists the metal ligands for 20 mononuclear Zn(II) enzymes, which are proposed to use a Zn(II)−hydroxide nucleophile. Of these, 12 have a +1 charge, 7 are neutral, and only 1 (cytidine deaminase) has a −1 charge, in the presence of hydroxide anion. Zn(II) metalloenzymes that catalyze alkylation of thiols incorporate the thiolate nucleophiles into negatively charged metal centers. These include the DNA repair Ada protein, which catalyzes alkylation of one of its own cysteine residues in a −2 Zn(II) center (*33*), *E. coli* cobalamin-independent methionine synthase at −1 or −2 (*47*), cobalamin-dependent methionine synthase thought to be at −2 (*48*), human betaine−homocysteine *S*-methyltransferase at −2 (*49*), and *Methanosarcina barkeri* methylcobamide: coenzyme M methyltransferases with possible net charges of −1 or −2 (*50*), where the net charges of the Zn(II) center are all given in the presence of ionized substrate thiol. The net charge of the zinc center for enzymes utilizing thiolate nucleophiles appears to reflect counterbalancing needs of using the metal to facilitate deprotonation of the thiol substrate, while permitting dissociation of the conjugate base from the inner coordination sphere of the zinc atom. During turnover PFTase binds FPP before the protein substrate. The FPP binding site contains several cationic groups (*51*) that may function to stabilize the development of negative charge by ionic interactions with or by protonation of the diphosphate as it leaves in the displacement reaction. While the protein can exclude large molecules from the active site, small molecules containing nucleophilic groups, such as glutathione, can enter and react with FPP, although at a much reduced rate (*37*). Because FPP binds tightly to PFTase (*36*, *52*), the binary PFTase·FPP complex is the predominant form of the enzyme in the cytosol (*53*). Thus, the bound molecule of FPP is potentially vulnerable to attack by a wide variety of small nucleophilic compounds or proteins with nucleophilic side chains in place of the CaaX cysteine. In addition, proteins with non-cysteine-containing C-terminal motifs that resemble the CaaX structure compete with the normal protein substrates for binding.

The Zn(II)(his)(asp)(cys) center in the enzyme helps to guard against nonspecific prenylation and inhibition by cellular proteins not targeted for prenylation by providing an environment that is specifically tuned to deprotonate thiol groups. For example, PFTase is not active toward peptides containing SaaX motifs (*2*, *54*), and we found that the corresponding β-aminoalanine analogues are also not substrates. These peptides are also poor inhibitors. Presumably, the hydroxyl and amino groups do not interact strongly with the zinc. In addition, PFTase does not catalyze hydrolysis of FPP. In contrast, farnesyl diphosphate synthase, a prenyltransferase that catalyzes alkylation of carbon−carbon double bonds by allylic diphosphates, will slowly hydrolyze its allylic substrate (*55*). A similar hydrolysis reaction for PFTase would waste FPP by slowly turning over the binary PFTase·FPP complex. Although small thiol-containing molecules are alkylated by FPP, the catalytic efficiencies of these reactions are very low (*37*). Thus, PFTase uses two filters to prevent farnesylation of extraneous nucleophiles. Selective binding discriminates against alkylation of small nonpeptidic cellular thiols, and selective activation discriminates against nonthiolate nucleophiles. It is interesting to note that the chemical selectivity can only be maintained if the prenylation reaction proceeds through an associative transition state. The allylic carbocation generated in a dissociative reaction is sufficiently reactive to alkylate a wide variety of nucleophiles, including those as weak as carbon−carbon double bonds (*56*). The effect of the net charge of the Zn(II) center on k_{cat} for wt PFTase and those mutants with measurable activity is summarized in Table 4. There was a general trend for k_{cat} to increase as the charge at the Zn(II) center of the enzyme·FPP·protein complex decreased. Although the inactive H363C 2− mutant did not follow this trend, two other 2− mutants, H363E and 3Cys, were active. A similar trend was reported for the rate of demethylation of trimethyl phosphate by Zn(II) methylimidazole/benzenethiolate complexes in model studies (*44*, *45*).

The activities of the mutant PFTases were also effected by structural factors not related to the charge at the Zn(II) center. This is easily seen by comparing the k_{cat}s for wt PFTase and the D307C mutant, with a net charge of −1, and the H363C and 3Cys mutants, with a net charge of −2. This observation is not surprising in view of the optimization of wt PFTase that has occurred through evolution and the differences between the geometries of the amino acids in the wt and mutant enzymes. A similar scatter of activities was seen for carbonic anhydrase mutants upon mutation of the amino acids ligated to Zn(II), where crystal structures were particularly instructive. In some cases structural distortions in the vicinity of the catalytic site were so severe that the amino acid replacement was displaced by a water molecule in the inner coordination sphere of the Zn(II) atom (*57*). An X-ray structure is not available for yeast PFTase, and our own attempts to produce crystals have failed, nor were we able to obtain Co(II) PFTase for UV measurements by reconstitution of the apoenzyme.

In their model study, Wilker and Lippard concluded that a thiolate produced by dissociation of the Zn(II) complex was the reactive species in the demethylation of trimethyl phosphate (*45*). Increases in the rate of demethylation seen as the net charge of the Zn(II) complex became more negative were attributed to increases in the equilibrium concentration of the free thiolate. A related mechanism, where the reactive thiolate dissociates from the Zn(II) atom prior to reacting with FPP, might resolve a paradox in the X-ray structure of a PFTase·peptide·(FPP analogue) complex. In work with the human enzyme, the distance from the Zn(II)-bound peptide thiolate to C1 of an FPP analogue was 7 Å in the ternary complex (*18*). This is well beyond the optimal distance for an associative displacement. Either the enzyme undergoes a substantial conformational change not seen in the X-ray structure that brings the Zn(II)-bound thiolate and FPP closer or the peptide thiolate dissociates from Zn(II) prior to the displacement of PP_i from FPP. In any event, the structure of the Zn(II) center is a crucial part of the catalytic machinery of PFTase and appears to be tuned

to facilitate deprotonation of the thiol moiety in the protein substrates for the subsequent nucleophilic displacement without activating less acidic groups. This selectivity might be an important factor in allowing PFTase to discriminate between cysteine and serine residues.

ACKNOWLEDGMENT

The authors thank Drs. Andrea Haemmerlin and Julie Kadrmas for helpful discussions.

REFERENCES

1. Harris, C. M., and Poulter, C. D. (2000) *Nat. Prod. Rep. 17*, 137−144.
2. Moores, S. L., Schaber, M. D., Mosser, S. D., Rands, E., O'Hara, M. B., Garsky, V. M., Marshall, M. S., Pompliano, D. L., and Gibbs, J. B. (1991) *J. Biol. Chem. 266*, 14603−14610.
3. Yokoyama, K., Goodwin, G. W., Ghomashchi, F., Glomset, J. A., and Gelb, M. H. (1991) *Proc. Natl. Acad. Sci. U.S.A. 88*, 5302−5306.
4. Horiuchi, H., Kawata, M., Katayama, M., Yoshida, Y., Musha, T., Ando, S., and Takai, Y. (1991) *J. Biol. Chem. 266*, 16981−16984.
5. Cox, A. D., and Der, C. J. (1997) *Biochim. Biophys. Acta 1333*, F51−F71.
6. Casey, P. J., Solski, P. A., Der, C. J., and Buss, J. E. (1989) *Proc. Natl. Acad. Sci. U.S.A. 86*, 8323−8327.
7. Hancock, J. F., Magee, A. I., Childs, J. E., and Marshall, C. J. (1989) *Cell 57*, 1167−1177.
8. Schafer, W. R., Kim, R., Sterne, R., Thorner, J., Kim, S.-H., and Rine, J. (1989) *Science 245*, 379−385.
9. Jackson, J. H., Cochrane, C. G., Bourne, J. R., Solski, P. A., Buss, J. E., and Der, C. J. (1990) *Proc. Natl. Acad. Sci. U.S.A. 87*, 3042−3046.
10. Adjei, A. A., Erlichman, C., Davis, J. N., Cutler, D. L., Sloan, J. A., Marks, R. S., Hanson, L. J., Svingen, P. A., Atherton, P., Bishop, W. R., Kirschmeier, P., and Kaufmann, S. H. (2000) *Cancer Res. 60*, 1871−1877.
11. Eskens, F. A., Awada, A., Cutler, D. L., de Jonge, M. J., Luyten, G. P., Faber, M. N., Statkevich, P., Sparreboom, A., Verweij, J., Hanauske, A. R., and Piccart, M. (2001) *J. Clin. Oncol. 19*, 1167−1175.
12. Karp, J. E., Lancet, J. E., Kaufmann, S. H., End, D. W., Wright, J. J., Bol, K., Horak, I., Tidwell, M. L., Liesveld, J., Kottke, T. J., Ange, D., Buddharaju, L., Gojo, I., Highsmith, W. E., Belly, R. T., Hohl, R. J., Rybak, M. E., Thibault, A., and Rosenblatt, J. (2001) *Blood 97*, 3361−3369.
13. Reiss, Y., Brown, M. S., and Goldstein, J. L. (1992) *J. Biol. Chem. 267*, 6403−6408.
14. Chen, W. J., Moomaw, J. F., Overton, L., Kost, T. A., and Casey, P. J. (1993) *J. Biol. Chem. 268*, 9675−9680.
15. Dolence, J. M., Rozema, D. B., and Poulter, C. D. (1997) *Biochemistry 36*, 9246−9252.
16. Park, H.-W., Boduluri, S. R., Moomaw, J. F., Casey, P. J., and Beese, L. S. (1997) *Science 275*, 1800−1804.
17. Huang, C.-C., Casey, P. J., and Fierke, C. A. (1997) *J. Biol. Chem. 272*, 20−23.
18. Strickland, C. L., Windsor, W. T., Syto, R., Wang, L., Bond, R., Wu, Z., Schwartz, J., Le, H. V., Beese, L. S., and Weber, P. C. (1998) *Biochemistry 37*, 16601−16611.
19. Hightower, K. E., Huang, C.-C., Casey, P. J., and Fierke, C. A. (1998) *Biochemistry 37*, 15555-15562.
20. Rozema, D. B., and Poulter, C. D. (1999) *Biochemistry 38*, 13138−13146.
21. Bertini, I., Luchinat, C., Rosi, M., Sgamellotti, A., and Tarantelli, F. (1990) *Inorg. Chem. 29*, 1460−1463.
22. Pocker, Y., and Bjorkquist, D. W. (1977) *Biochemistry 16*, 5698−5707.
23. Kiefer, L. L., and Fierke, C. A. (1994) *Biochemistry 33*, 15233−15240.
24. Davisson, V. J., Woodside, A. B., and Poulter, C. D. (1986) *Methods Enzymol. 110*, 130−144.
25. Mayer, M. P., Prestwich, G. D., Dolence, J. M., Bond, P. D., Wu, H.-Y., and Poulter, C. D. (1993) *Gene 132*, 41−47.
26. Pompliano, D. L., Gomez, R. P., and Anthony, N. J. (1992) *J. Am. Chem. Soc. 114*, 7945−7946.
27. Cassidy, P. B., Dolence, J. M., and Poulter, C. D. (1995) *Methods Enzymol. 250*, 30−43.
28. Dolence, J. M., Cassidy, P. B., Mathis, J. R., and Poulter, C. D. (1995) *Proc. Natl. Acad. Sci. U.S.A. 92*, 5008−5011.
29. Silverman, D. N., and Lindskog, S. (1988) *Acc. Chem. Res. 21*, 30−36.
30. Christianson, D. W., and Lipscomb, W. N. (1989) *Acc. Chem. Res. 22*, 62−69.
31. Eklund, H., and Branden, C.-I. (1983) in *Zinc Enzymes* (Spiro, T. G., Ed.) pp 123−152, John Wiley and Sons, New York.
32. Wilson, D. K., Rudolph, F. B., and Quiocho, F. A. (1991) *Science 252*, 1278−1284.
33. Myers, L. C., Verdine, G. L., and Wagner, G. (1993) *Biochemistry 32*, 14089−14094.
34. Zimmerman, K. K., Scholten, J. D., Huang, C. C., Fierke, C. A., and Hupe, D. J. (1998) *Protein Expression Purif. 14*, 395−402.
35. Wu, Z., Demma, M., Strickland, C. L., Syto, R., Le, H. V., Windsor, W. T., and Weber, P. C. (1999) *Protein Eng. 12*, 341−348.
36. Mathis, J. R., and Poulter, C. D. (1997) *Biochemistry 36*, 6367−6376.
37. Hightower, K. E., Casey, P. J., and Fierke, C. A. (2001) *Biochemistry 40*, 1002−1010.
38. Frausto da Silva, J. J. R., and Williams, R. J. P. (1991) in *The Biological Chemistry of the Elements*, pp 299−303, Clarendon Press, Oxford.
39. Dreyer, M. K., and Schulz, G. E. (1996) *J. Mol. Biol. 259*, 458−466.
40. Wilson, D. K., and Quiocho, F. A. (1993) *Biochemistry 32*, 1689−1694.
41. Kim, E. E., and Wyckoff, H. W. (1991) *J. Mol. Biol. 218*, 449−464.
42. Roberts, D. D., Lewis, S. D., Ballou, D. P., Olson, S. T., and Shafer, J. A. (1986) *Biochemistry 25*, 5595−5601.
43. Mayr, H., and Patz, M. (1994) *Angew. Chem., Int. Ed. Engl. 33*, 938−957.
44. Wilker, J. J., and Lippard, S. J. (1995) *J. Am. Chem. Soc. 117*, 8682−8683.
45. Wilker, J. J., and Lippard, S. J. (1997) *Inorg. Chem. 36*, 969−978.
46. Lipscomb, W. N., and Strater, N. (1996) *Chem. Rev. 96*, 2375−2433.
47. Gonzalez, J. C., Peariso, K., Penner-Hahn, J. E., and Matthews, R. G. (1996) *Biochemistry 35*, 12228−12234.
48. Peariso, K., Goulding, C. W., Huang, S., Matthews, R. G., and Penner-Hahn, J. E. (1998) *J. Am. Chem. Soc. 120*, 8410−8416.
49. Breksa, A. P., and Garrow, T. A. (1999) *Biochemistry 38*, 13991−13998.
50. LeClerc, G. M., and Grahame, D. A. (1996) *J. Biol. Chem. 271*, 18725−18731.
51. Long, S. B., Casey, P. J., and Beese, L. S. (1998) *Biochemistry 37*, 9612−9618.
52. Furfine, E. S., Leban, J. J., Landavazo, A., Moomaw, J. F., and Casey, P. J. (1995) *Biochemistry 34*, 6857−6862.
53. Bruenger, E., and Rilling, H. C. (1988) *Anal. Biochem. 173*, 321−327.
54. Goldstein, J. L., Brown, M. S., Stradley, S. J., Reiss, Y., and Gierasch, L. M. (1991) *J. Biol. Chem. 266*, 15575−15578.
55. Poulter, C. D., and Rilling, H. C. (1976) *Biochemistry 15*, 1079−1083.
56. Cane, D. E. (1999) in *Comprehensive Natural Products Chemistry* (Barton, D., Nakanishi, K., and Meth-Cohn, O., Eds.) Vol. 2, pp 4−11, Elsevier Science Ltd., Oxford.
57. Ippolito, J. A., and Christianson, D. W. (1994) *Biochemistry 33*, 15241−15249.

BI020349U